

## Research Article

# Preparation and Properties of Nanocellulose from *Miscanthus x giganteus*

Valerii A. Barbash , Olha V. Yashchenko, and Olesia A. Vasylieva

Department of Ecology and Technology of Plant Polymers, Igor Sikorsky Kyiv Polytechnic Institute, Prospect Peremohy, 37 Kyiv 03056, Ukraine

Correspondence should be addressed to Valerii A. Barbash; v.barbash@kpi.ua

Received 30 August 2019; Accepted 28 October 2019; Published 12 November 2019

Academic Editor: Sessa Srinivasan

Copyright © 2019 Valerii A. Barbash et al. This is an open access article distributed under the Creative Commons Attribution License, which permits unrestricted use, distribution, and reproduction in any medium, provided the original work is properly cited.

*Miscanthus x giganteus* stalks were used to make organosolvent pulp and nanocellulose. The organosolvent miscanthus pulp (OMP) was obtained through thermal treatment in the mixture of glacial acetic acid and hydrogen peroxide at the first stage and the alkaline treatment at the second stage. Hydrolysis of the never-dried OMP was carried out by a solution of sulfuric acid with concentrations of 43% and 50% and followed by ultrasound treatment. Structural changes and the crystallinity index of OMP and nanocellulose were studied by SEM and FTIR methods. X-ray diffraction analysis confirmed an increase in the crystallinity of OMP and nanocellulose as a result of thermochemical treatment. We show that nanocellulose has a density of up to 1.6 g/cm<sup>3</sup>, transparency up to 82%, and a crystallinity index of 76.5%. The AFM method showed that the particles of nanocellulose have a diameter in the range from 10 to 20 nm. A thermogravimetric analysis confirmed that nanocellulose films have a denser structure and lower mass loss in the temperature range of 320–440°C compared to OMP. The obtained nanocellulose films have high tensile strength up to 195 MPa. The nanocellulose obtained from OMP exhibits the improved properties for the preparation of new nanocomposite materials.

## 1. Introduction

Industrial developments, as well as changing consumption patterns associated with growing economies and prosperity, contribute to increasing demand for both renewable biological resources and nonrenewable stocks of minerals, metals, and fossil fuels. The limited reserves of mineral resources (oil, gas, and coal) determine the relevance of research in technologies for producing biodegradable materials from the renewable sources of raw materials [1]. Such renewable resources include raw plant materials, the products from the treatment of which have found wide use in various industries: chemical, pharmaceutical, paper, textile, electronic, and others [2, 3]. The main component of plant materials is cellulose, the most common biopolymer in nature. Cellulose is used for the production of nanocellulose and composite materials.

Nanocellulose is a new class of nanomaterials, which has unique properties, such as nanoscalability and biocompati-

bility and being a renewable and biodegradable material, that enable its use in many fields [4, 5]. Nanocellulose is used in optoelectronics, in the production of chemical current of sources and sorbents, for reinforcing and improving the thermal stability of polymeric and paper composites [6–8]. Nanocellulose has been incorporated into polymer matrices to produce reinforced composites of tenfold to hundredfold mechanical strength [9], as well as enhanced optical transparency [10]. These specific characteristics of nanocellulose reinforce mechanical properties of the polymer and improve the film's mechanical and/or barrier properties [11, 12].

Nanocellulose is obtained by acid hydrolysis and mechanical, oxidative, and enzymatic treatments of cellulose fibers [13–15]. The chemical method of hydrolysis of cellulose by acid solutions is the most common technique [16]. Usually, nanocellulose is obtained by acid hydrolysis of cellulosic materials from wood and nonwood plants. The main raw material used to produce cellulose on a worldwide scale is wood. The search for alternative sources of plant materials

continues to be a priority in countries where wood is scarce as a natural resource. Nonwood plants are a good candidate for an alternative source of such raw materials in the production of pulp.

In our previous works, we described the technology for obtaining nanocellulose from wheat straw [17], flax [18], and kenaf [19] and its properties. In the current work, we describe the conditions for obtaining nanocellulose from *Miscanthus x giganteus*, which is widely cultivated in Europe and the United States. *Miscanthus giganteus* (*Miscanthus x giganteus*) is a fast-growing perennial herb that grows in the European climatic zone, quite unpretentious and inexpensive to grow, with a high content of cellulose up to 49.7% [20]. *Miscanthus* is quite resistant to diseases, has frost resistance, and has rapid growth. The yield of miscanthus can reach 10–35 dry tons per hectare, and after a single planting, culture can be collected annually for 15–20 years [21]. Compared to wood, which requires about 10–12 years to fully mature, miscanthus requires a maximum of 3 years after planting to reach its peak dry biomass production which further showcases its potential as a viable source of raw materials. It is also one of the few plant species being dedicated to biomass cropping and is currently farmed in Europe and the United States primarily for use in electricity and heat generation (by combustion) as well as feedstock for biofuels. More recently, miscanthus has been expanded into other markets such as advanced materials and biobased products [22]. We characterize the organosolvent pulp obtained from the miscanthus using an environmentally safer method and the nanocellulose that can be obtained from it, and we also report on the properties of this nanocellulose.

## 2. Materials and Methods

**2.1. Raw Material and Chemicals.** We used the second-year miscanthus biomass as feedstock. The plant was grown in 2016–2017 in the grey-forest soil at the research field in Kyiv's vicinity. *Miscanthus* stalks were cleaned of leaves and nodes, crushed into particles of 5–7 mm in size and placed in a desiccator to maintain constant moisture and chemical composition. The chemical composition of miscanthus was determined according to TAPPI standards [23], namely, T 222 for lignin, T 257 for substances extracted with hot water, T 212 for substances extracted with 1% solution of NaOH, T 204 for substances extracted with alcohol-benzene solution, and T 211 to determine ash content and cellulose by the Kurschner-Hoffer method. All chemicals, including ice acetic acid, 35% hydrogen peroxide, NaOH, and sulfuric acid, were produced in Ukraine and used without further purification.

**2.2. Obtaining Pulp.** Cooking of miscanthus pulp was carried out in two stages. At the first stage, treatment of *Miscanthus x giganteus* in a mixture of glacial acetic acid and 35% hydrogen peroxide in a volume ratio of 70:30% at the liquid to solid ratio 10:1, at a temperature of  $95 \pm 2^\circ\text{C}$  for 30–240 min, was carried out. The cooking regime was determined in previous studies [17–19].

At the second stage, the alkaline treatment of obtained organosolvent miscanthus pulp (OMP) by solution of NaOH concentration of 7% for 15–240 min, at the liquid to solid ratio 12:1 at a temperature of  $95 \pm 2^\circ\text{C}$ , was carried out. The OMP after alkaline treatment was washed with hot distilled water to a neutral pH and was stored in sealed bags in a refrigerator for further research. The quality parameters of the obtained OMP samples we determined according to standard methods [23].

**2.3. Obtaining Nanocellulose.** Hydrolysis of the never-dried OMP was carried out by solution of sulfuric acid with concentrations of 43 and 50%, at the liquid to solid ratio 10:1, at temperatures of 40 and  $60^\circ\text{C}$  for 30–90 min, to obtain nanocellulose. The calculated amount of sulfate acid with the corresponding concentration was slowly added into the flask with the OMP suspension. Upon expiration of the reaction time, the hydrolysis was stopped by tenfold dilution with distilled water and cooling of the suspension to room temperature. The hydrolyzed nanocellulose was rinsed with distilled water three times by means of centrifugation at 4000 rev/min and subsequent dialysis until reaching neutral pH. Ultrasound treatment of nanocellulose with a concentration of 0.6% was performed using an ultrasound disintegrator UZDN-A (SEMI, Ukraine) with 22 kHz from 30 to 60 min. The nanocellulose suspension was placed in an ice bath to prevent overheating during treatment.

**2.4. Methods of Analyses.** The following instrumental methods of analysis of plant raw material, organosolvent miscanthus pulp, and nanocellulose have been used. The decrease of the cellulose particle size and the increase of its dispersity were assessed by measuring the changes in the dimensions of the miscanthus pulp. Scanning electron microscope (SEM) analysis was performed with a PEM-106I (SEMI, Ukraine) microscope to observe the morphology of OMP and nanocellulose films.

Topographical characterization of nanocellulose samples was assessed by atomic force microscopy (AFM). The measurements were done with a Si cantilever, operating in the tapping mode on the device Solver Pro M (NT-MDT, Russia). Details of the measurements are described in article [17].

X-ray diffraction patterns of the different cellulose samples were obtained by an Ultima IV diffractometer (Rigaku, Japan). Crystallinity index (CI) was used to calculate relative amount of crystalline material in the cellulose by the Segal method [24]:  $\text{CI} = (I_{200} - I_{\text{am}})/I_{200} \times 100\%$ , where  $I_{200}$  is the intensity of (200) reflex about  $23^\circ$  and  $I_{\text{am}}$  is the intensity of amorphous scattering at  $18.5^\circ$ .

Electron absorption spectra of the nanocellulose films in UV, visible, and near-infrared regions were registered on a two-beam spectrophotometer 4802 (UNICO, USA) with a resolution of 1 nm.

The thermal degradation behavior of OMP, OMP after alkaline treatment, and nanocellulose samples was studied on a Q-1500D thermal analyzer (F. Paulik, J. Paulik, L. Erdey system, Hungary) from 25 to  $600^\circ\text{C}$  with a heating rate of  $5^\circ\text{C min}^{-1}$ . The weight of samples was within 0.25

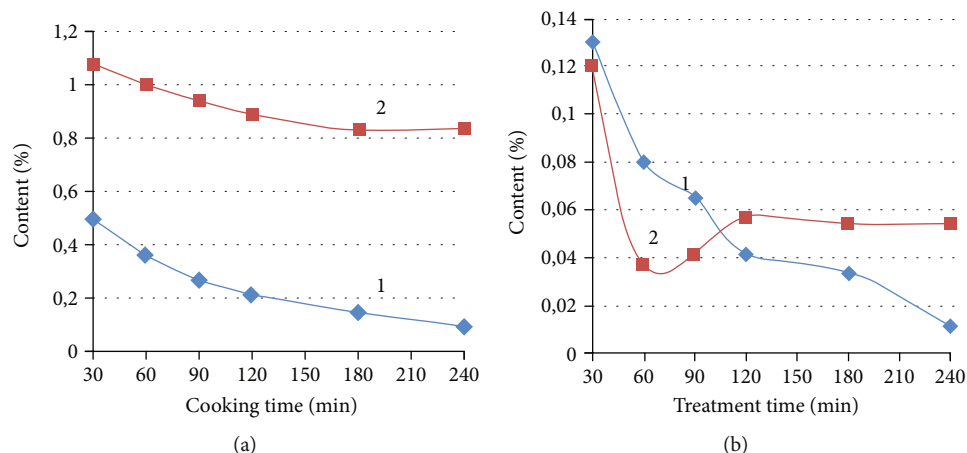


FIGURE 1: Properties of organosolvent miscanthus pulp after cooking (a) and alkaline treatment (b), % to a.d.r.m. 1: residual lignin; 2: ash content.

$\pm 0.01$  grams, reference substance— $\alpha$ -corundum, crucible material—alund. Deviations of weight were registered and processed according to a program involving the use of computer technology.

Functional groups of OMP, OMP after alkaline treatment, and nanocellulose samples were analyzed using Fourier transform infrared spectrophotometer (FTIR Spectrometer “Tensor 37”) in the range of  $4000\text{--}500\text{ cm}^{-1}$  with a resolution of  $2\text{ cm}^{-1}$ .

The density of the nanocellulose films was determined in accordance with ISO 534:1988. Tensile strength of the nanocellulose films was measured at a controlled temperature of  $23 \pm 1^\circ\text{C}$  and humidity of  $50 \pm 2\%$  according to ISO 527-1 as described in [17].

### 3. Results and Discussion

**3.1. Results of Cooking and Alkali Treatment.** Miscanthus stalks had the following chemical composition: 49.7% of cellulose; 27.7% of lignin; 1.8% of resins, fats, and waxes; 61.9% of pentosans; and 1.1% of mineral substances relative to absolutely dry raw material (a.d.r.m.). As can be seen from the chemical composition data, the miscanthus stalks according to the content of the main components—cellulose and lignin—correspond to softwood but contain more mineral substances than softwood and hardwood. The analysis of the content of the main components of miscanthus a priori allows us to conclude that this raw material can be considered to produce both pulp suitable for paper and cardboard and pulp for chemical processing, in particular, for the production of nanocellulose.

An increase in the cooking time from 30 to 240 minutes naturally leads to a decrease in the yield of pulp from 54.3% to 45.7% to a.d.r.m. Figure 1 shows the dependence of the content of lignin (1) and mineral substances (2) on the processing time.

As shown in Figure 1(a), the mineral content in the organosolvent miscanthus pulp after 90 minutes of cooking does not significantly decrease and remains in the range of 0.84–0.95% to a.d.r.m. Therefore, after 90 minutes of cooking, cel-

lulose was used for its subsequent alkaline treatment in order to reduce the content of minerals and lignin in it. Figure 1(b) shows the dependence of contents of lignin (1) and mineral substances (2) in the pulp after the alkaline treatment. As a result of experiments, it was found that increasing the duration of the alkaline treatment from 30 to 240 minutes reduces the pulp yield from 72.3% to 51.0% to a.d.r.m. Subsequent alkaline treatment does not contribute to the extraction of minerals, but rather, the polysaccharides dissolve, the yield of pulp decreases, and, therefore, the percentage of ash increases. Therefore, to prepare nanocellulose from organosolvent pulp, we used 90-minute cooking and alkaline treatment for 60 minutes with a lignin content of 0.08% and mineral substances of 0.037% to a.d.r.m. Thus, carrying out peroxide cooking and alkaline treatment at low temperature ( $96 \pm 1^\circ\text{C}$ ) allows obtaining of cellulose with a high degree of whiteness (up to 85%) and low emissions of harmful substances into the environment.

**3.2. SEM Analysis.** The morphology structure of the samples of the miscanthus and organosolvent miscanthus pulp before and after alkaline treatment is shown in Figure 2.

The main components are xylem cells and phloem, which perform the conductive, mechanical, and storage functions in the stalks of plants. These include cells of tracheids, vessels, libriform, and parenchymal cells (Figure 2(a)). The presence of such cells is typical for different representatives of non-wood plant materials. The walls of miscanthus stalks consist of a network of longitudinal oval capillaries that provide access to the cooking solution to the cells. As a result of cooking, the miscanthus is exposed to thermochemical effects and the stalks are folded into separate short and wide fragments (Figure 2(b)). According to the SEM, the bulk of the pulp from miscanthus is made up of thin, ribbon fibers of different widths and lengths and can be single and joined to several pieces. The photographs confirm that in the process of thermochemical processing of plant materials, the size of the fibers decreases, primarily their width due to the removal of noncellulose plant components from them. Moreover, as can be seen from Figure 2(c), the fiber after intensive alkaline

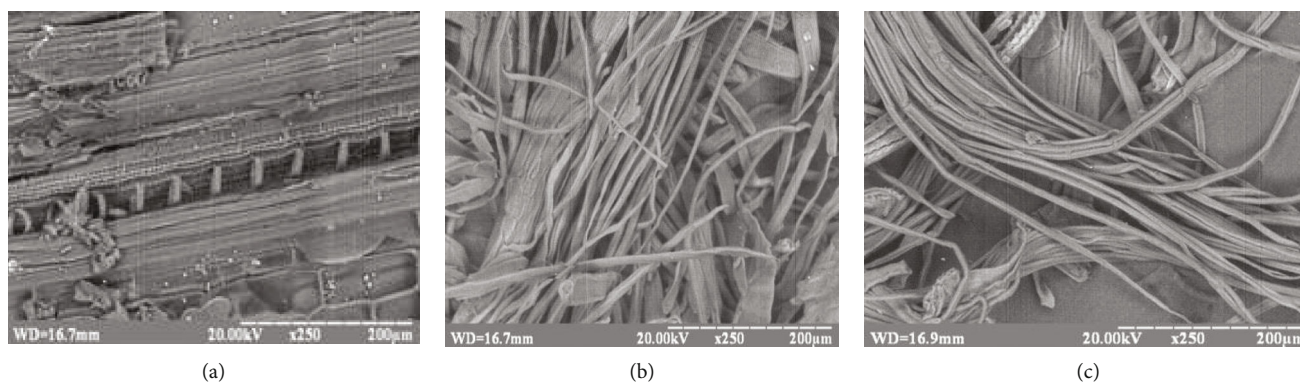


FIGURE 2: Scanning electron microscopy images of samples of the miscanthus stalks (a) and organosolvent miscanthus pulp before (b) and after alkaline treatment (c).

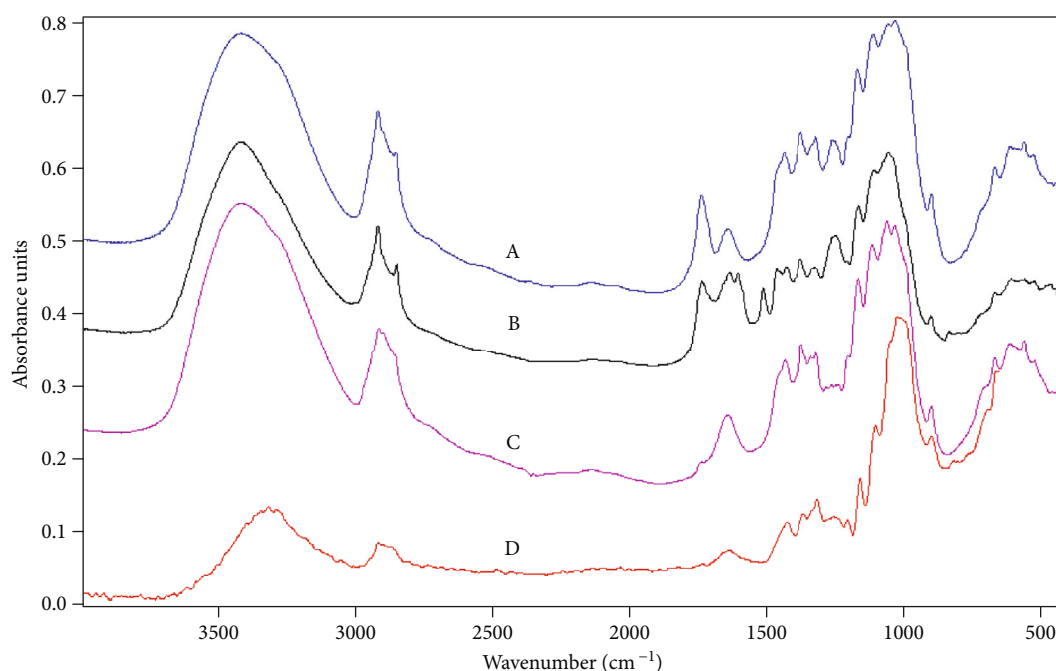


FIGURE 3: FTIR spectra of different samples: of miscanthus stalks (A), organosolvent miscanthus pulp before (B) and after alkaline treatment (C), and nanocellulose film (D).

treatment has a smooth surface, which indicates the relative chemical purity of the cellulose fibers.

**3.3. FTIR Analysis.** The extraction of noncellulosic components from organosolvent miscanthus pulp in the process of its thermochemical treatment was confirmed by infrared spectroscopy. Figure 3 shows the Fourier IR spectra of the miscanthus stalks, organosolvent miscanthus pulp before and after alkaline treatment, and the nanocellulose after hydrolysis.

All spectra are characterized by a wide bandwidth in the region of  $3000\text{--}3800\text{ cm}^{-1}$ , which corresponds to stretching vibrations of hydroxyl groups included in intramolecular and intermolecular hydrogen bonds [24]. Spectra of miscanthus stalks and organosolvent miscanthus pulp before and after alkaline treatment have characteristic high-

frequency bands, indicating the formation of intermolecular bonds. The band of nanocellulose in this region is characterized by low intensity, which indicates the formation of strong intermolecular bonds between the hydroxyl groups of the macromolecules of nanocellulose. The bands in the area of  $3000\text{--}2800\text{ cm}^{-1}$  correspond to the asymmetric and symmetric stretching vibrations of the methylene groups of the cellulose. Bands of stretching vibrations of double bonds lie in the region of  $1500\text{--}1800\text{ cm}^{-1}$ . Vibration bands in the  $1740\text{ cm}^{-1}$  region indicate the presence of a carbonyl group characteristic of hemicelluloses. As can be seen from Figure 3, C, organosolvent cooking and subsequent alkaline treatment removes hemicelluloses from the cellulose composition. A decrease in the intensity of vibrations in the region of  $1600\text{ cm}^{-1}$ , which is characteristic of aromatic compounds—residual lignin, indicates an almost complete

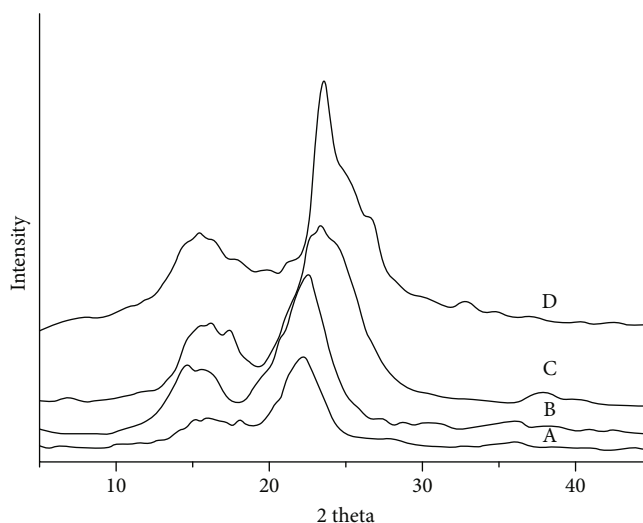


FIGURE 4: X-ray diffraction patterns of different cellulose samples: (A) miscanthus stalks, (B) organosolvent pulp, (C) OMP after alkaline treatment, and (D) nanocellulose after hydrolysis and sonication.

removal of lignin from plant materials and cellulose during their thermochemical treatments. The bands in the region of  $1370$  and  $1430\text{ cm}^{-1}$  are due to the deformation vibrations of the  $\text{CH}_2$  groups, the band at  $1160\text{ cm}^{-1}$  is due to the asymmetric vibrations of the  $\text{C}-\text{O}$  bonds, while the band at  $1060\text{ cm}^{-1}$  corresponds to the vibrations of the  $\text{C}-\text{O}-\text{C}$  bridge of the glucopyranose ring of cellulose [25]. The increase of the intensity of the bands in the region of  $1050$ ,  $1400$ , and  $3400\text{ cm}^{-1}$  demonstrates the efficiency of the removal of lignin and noncellulose components from the plant feedstock in the investigated sequence of thermochemical treatments.

**3.4. XRD Analysis.** The change in the ratio of amorphous and crystalline parts of OMP during its thermochemical and physical treatment was investigated by the XRD method. The analysis of X-ray diffraction patterns of miscanthus stalks (Figure 4, A), organosolvent miscanthus pulp (Figure 4, B), OMP after alkaline treatment (Figure 4, C), and nanocellulose after hydrolysis and sonication (Figure 4, D) was carried out.

The crystallinity index of miscanthus stalks was 65.8%; organosolvent pulp, 72.3%; OMP after alkaline treatment, 71.9%; and nanocellulose after hydrolysis and sonication, 76.7%. Thus, the results of X-ray diffraction analysis indicate an increase in the sample crystallinity in the process of their thermochemical and physical processing. This dependence is observed for cellulose from other representatives of nonwood and woody plant raw materials [17–19, 26, 27].

**3.5. Results of Hydrolysis.** We show the dependencies of the density, tensile strength, and transparency of nanocellulose films on the main technological parameters of the process for obtaining nanocellulose from organosolvent miscanthus pulp (Table 1). As can be seen from the data in Table 1, the hydrolysis of cellulose by solutions of sulfuric acid of different concentrations yields nanocellulose films of different quality. An increase in the quality of nanocellulose films

improves with increasing sulfuric acid concentration, temperature, and duration of hydrolysis. An increase in the duration of ultrasonic treatment of suspension of nanocellulose obtained within one time of hydrolysis from 30 to 60 minutes increases the strength and transparency of nanocellulosic films. The highest values of quality indicators are the samples obtained at the maximum values of the studied technological parameters. The values of transparency of the films prepared in this study are higher than the transparency of the cellulose nanofiber films obtained from bleached kraft eucalyptus, acacia, and pine pulps reported previously (40–65%) [28].

The properties of obtained nanocellulose from OMP exhibit great potential in its application for the preparation of new nanocomposite materials, for example, for production in optoelectronic devices, as a reinforcing additive in the production of paper, cardboard, cement, etc.

Nanocellulose after hydrolysis and ultrasound treatment of OMP had homogeneous and stable nanocellulose suspension. The nature of stabilization of the colloidal suspension is explained by the presence of charged groups on the surface of the nanocellulose, which are formed by the interaction of cellulose with sulfuric acid due to the esterification reaction. The stability of nanocellulose suspensions is supported by images immediately after the preparation and after a prolonged storage time. There was no sedimentation of nanocellulose particles when stored at room temperature for an extended period of time (after 5 months of storage). Such stabilization of the nanocellulose suspension leads to the formation of films with a transparency of more than 80% in the visible spectral range, which is confirmed by the data of the article [29] and characteristic of nanocellulose from other plant raw materials [27].

**3.6. AFM Analyses.** Topographical characterization of organosolvent miscanthus nanocellulose by AFM and its 3D projection with definition of sample height is shown in Figure 5.

Figure 5(a) shows the lateral section of the miscanthus nanocellulose nanofibers, which form aggregates. The diameter of separate nanofibers is within the range from

TABLE 1: Dependencies of the parameters of nanocellulose films on the main technological parameters of the process of obtaining nanocellulose from organosolvent miscanthus pulp.

Concentration H <sub>2</sub> SO <sub>4</sub> (%)	Duration of hydrolysis (min)	Duration of ultrasonic treatment (min)	Density (g/cm <sup>3</sup> )	Quality of received films	
				Tensile strength (MPa)	Transparency (%)
Temperature 40°C					
43/50	30	30	0.87/1.00	56.0/44.2	25.8/57.0
		45	1.04/1.08	58.3/54.1	40.6/64.2
		60	1.05/1.12	80.0/66.7	41.8/67.0
	60	30	1.04/1.12	54.5/50.0	30.3/51.1
		45	1.08/1.15	59.3/66.1	43.3/67.0
		60	1.16/1.22	77.7/83.3	52.7/69.7
	90	30	1.09/1.15	70.7/77.5	42.7/59.9
		45	1.11/1.18	83.3/105.0	54.5/64.3
		60	1.18/1.23	124.0/127.0	55.6/69.3
Temperature 60°C					
43/50	30	30	1.12/1.1	43.3/66.7	44.3/65.7
		45	1.22/1.23	57.5/70.7	52.0/75.6
		60	1.26/1.28	60.4/75.0	70.7/76.3
	60	30	1.15/1.33	55.5/78.0	68.6/68.7
		45	1.23/1.37	60.0/80.6	65.3/70.9
		60	1.32/1.42	62.0/88.0	74.4/80.8
	90	30	1.04/1.45	44.4/115.0	38.5/75.7
		45	1.18/1.55	40.0/123.0	68.2/78.0
		60	1.25/1.60	41.0/195.0	72.3/82.6

10 to 20 nm and possibly much less, since the image is obtained from fibers of nanocellulose located not in one layer. Therefore, we propose that the nanocellulose forms a film on the surface of the silicon substrate due to bonds between the molecules.

**3.7. TGA and DTA Analyses.** We also investigated the change in the thermal stability of samples of OMP, OMP after alkaline treatment, and nanocellulose films by the thermogravimetric analysis. Figure 6 shows the change of the thermal stability of OMP samples after cooking in peracetic acid (curve 1), of OMP after the alkaline treatment (curve 2), and of nanocellulose films after hydrolysis with 50% sulfuric acid and ultrasound treatment (curve 3).

As is shown in Figure 6, thermogravimetric curves of the studied samples have their own characteristics. So, in the temperature range from 50 to 90°C, the maximum weight loss (up to 12%) is observed for OMP, which is due to the evaporation of residual moisture from its fibers. When heating nanocellulose films to 240°C, and samples of OMP and OMP after alkaline treatment to 260°C, a slight (up to 3%) loss in mass is observed. In the process of further heating of the OMP and OMP samples after alkaline treatment to 340°C, up to 70% of their bulk is lost. Samples have a final degradation temperature of about 440°C for OMP and 500°C for OMP after alkaline treatment. For nanocellulose films, a smooth mass loss is observed in the temperature range 240–500°C, and the final decomposition is observed at a temperature of 540°C. It can be explained by the fact that during the

chemical treatment and ultrasonic homogenization, a dense structure between pulp molecules is formed. The degradation behavior of the cellulose that underwent sulfuric acid hydrolysis was different from that of the initial cellulose and showed higher degradation temperature. The higher degradation temperature of the nanocellulose was due to the formation of a dense crystalline structure of the cellulose. These end chains started to decompose at the lower temperatures, as have been previously shown [30]. Our data also support previous findings that the sulfate groups, introduced during hydrolysis, can work as a flame retardant in such a way that they cause an increase in the char fraction [31].

## 4. Conclusions

Based on our work, *Miscanthus x giganteus* is a promising plant raw material for the production of organosolvent pulp, suitable for chemical processing, in particular, for the production of nanocellulose. Carrying out peroxide cooking and alkaline treatment at low temperature  $96 \pm 1^\circ\text{C}$  allows obtaining organosolvent miscanthus pulp (OMP) with a high degree of whiteness up to 85% and low emissions of harmful substances into the environment. As a result of hydrolysis of never-dried cellulose with a solution of sulfuric acid with concentrations of 43 and 50% followed by ultrasonic treatment, nanocellulose was obtained. The structural changes and crystallinity degree of OMP and nanocellulose were studied by SEM and FTIR techniques. XRD analysis confirmed the increase of the degree of crystallinity of the

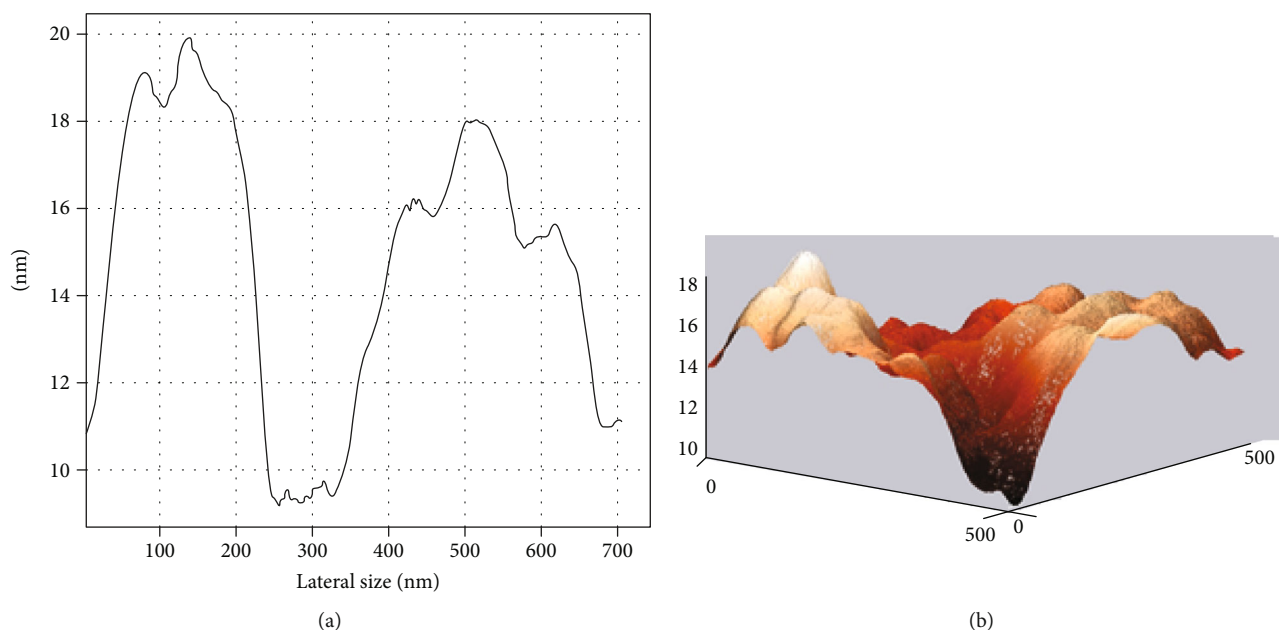


FIGURE 5: (a) The AFM images of the lateral size of the nanocellulose surface; (b) 3D projection with definition of sample height tapping mode.

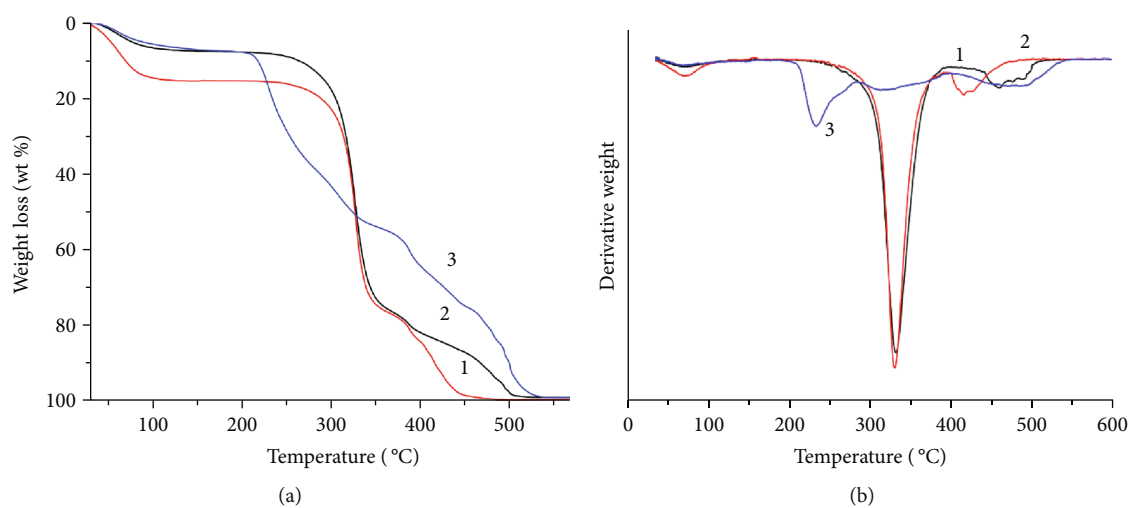


FIGURE 6: Gravimetric (a) and differential (b) curves of thermal analysis: (1) OMP, (2) OMP after alkaline treatment, and (3) nanocellulose film.

OMP and nanocellulose as a result of thermochemical treatment. We report that nanocellulose has a density up to  $1.6 \text{ g/cm}^3$ , transparency up to 82%, and crystallinity up to 76.5%. We observed using AFM microscopy that nanocellulose has a particle diameter in the range of 10 to 20 nm. Thermogravimetric analysis confirmed that nanocellulose films have a more dense structure and smaller mass loss in the temperature range of 320–440°C compared with OMP. Samples have a final degradation temperature of about 440°C for OMP and 500°C for OMP after alkaline treatment, but for nanocellulose films, the final decomposition is observed at a temperature of 540°C. The obtained nanocellulose films had high tensile strength up to 195 MPa. The properties of obtained nanocellulose from OMP exhibit great potential in

its application for the preparation of new nanocomposite materials and can serve reinforcing additive in paper, cardboard, cement, etc.

### Data Availability

The XRD, FTIR, and TGA data used to confirm the results of this study are included in additional information files that are attached.

### Conflicts of Interest

The authors declare that they have no conflicts of interest.

## Acknowledgments

This work was financially supported by the Ministry of Education and Science of Ukraine.

## References

- [1] R. Mülhaupt, "Green polymer chemistry and bio-based plastics: dreams and reality," *Macromolecular Chemistry and Physics*, vol. 214, no. 2, pp. 159–174, 2013.
- [2] H. P. S. A. Khalil, A. H. Bhat, and A. F. I. Yusra, "Green composites from sustainable cellulose nanofibrils: a review," *Carbohydrate Polymers*, vol. 87, no. 2, pp. 963–979, 2012.
- [3] Y. H. Jung, T.-H. Chang, H. Zhang et al., "High-performance green flexible electronics based on biodegradable cellulose nanofibril paper," *Nature Communications*, vol. 6, no. 1, 2015.
- [4] B. Deepa, E. Abraham, N. Cordeiro et al., "Utilization of various lignocellulosic biomass for the production of nanocellulose: a comparative study," *Cellulose*, vol. 22, no. 2, pp. 1075–1090, 2015.
- [5] K. Uetani, T. Okada, and H. T. Oyama, "Thermally conductive and optically transparent flexible films with surface-exposed nanocellulose skeletons," *Journal of Materials Chemistry C*, vol. 4, no. 41, pp. 9697–9703, 2016.
- [6] C. Wang, H. Huang, M. Jia, S. Jin, W. Zhao, and R. Cha, "Formulation and evaluation of nanocrystalline cellulose as a potential disintegrant," *Carbohydrate Polymers*, vol. 130, pp. 275–279, 2015.
- [7] S. Thiemann, S. J. Sachnov, F. Pettersson et al., "Cellulose-based ionogels for paper electronics," *Advanced Functional Materials*, vol. 24, no. 5, pp. 625–634, 2014.
- [8] A. M. Adel, A. A. El-Gendy, M. A. Diab, R. E. Abou-Zeid, W. K. El-Zawawy, and A. Dufresne, "Microfibrillated cellulose from agricultural residues. Part I: papermaking application," *Industrial Crops and Products*, vol. 93, pp. 161–174, 2016.
- [9] J. Luo, H. Chang, A. A. Bakhtiyari Davijani et al., "Influence of high loading of cellulose nanocrystals in polyacrylonitrile composite films," *Cellulose*, vol. 24, no. 4, pp. 1745–1758, 2017.
- [10] Y. Su, Y. Zhao, H. Zhang, X. Feng, L. Shi, and J. Fang, "Polydopamine functionalized transparent conductive cellulose nanopaper with long-term durability," *Journal of Materials Chemistry C*, vol. 5, no. 3, pp. 573–581, 2017.
- [11] K.-Y. Lee, Y. Aitomäki, L. A. Berglund, K. Oksman, and A. Bismarck, "On the use of nanocellulose as reinforcement in polymer matrix composites," *Composites Science and Technology*, vol. 105, pp. 15–27, 2014.
- [12] G. Siqueira, J. Bras, and A. Dufresne, "Cellulose whiskers versus microfibrils: influence of the nature of the nanoparticle and its surface functionalization on the thermal and mechanical properties of nanocomposites," *Biomacromolecules*, vol. 10, no. 2, pp. 425–432, 2009.
- [13] I. A. Sacui, R. C. Nieuwendaal, D. J. Burnett et al., "Comparison of the properties of cellulose nanocrystals and cellulose nanofibrils isolated from bacteria, tunicate, and wood processed using acid, enzymatic, mechanical, and oxidative methods," *ACS Applied Materials & Interfaces*, vol. 6, no. 9, pp. 6127–6138, 2014.
- [14] D. Y. Liu, G. X. Sui, and D. Bhattacharyya, "Synthesis and characterisation of nanocellulose-based polyaniline conducting films," *Composites Science and Technology*, vol. 99, pp. 31–36, 2014.
- [15] T. S. Anirudhan, J. R. Deepa, and Binusreejayan, "Synthesis and characterization of multi-carboxyl-functionalized nanocellulose/nanobentonite composite for the adsorption of uranium(VI) from aqueous solutions: Kinetic and equilibrium profiles," *Chemical Engineering Journal*, vol. 273, pp. 390–400, 2015.
- [16] J. Cruz and R. Figueiro, "Surface modification of natural fibers: a review," *Procedia Engineering*, vol. 155, pp. 285–288, 2016.
- [17] V. A. Barbash, O. V. Yaschenko, and O. M. Shnuruk, "Preparation and properties of nanocellulose from organosolv straw pulp," *Nanoscale Research Letters*, vol. 12, no. 1, p. 241, 2017.
- [18] V. Barbash, O. Yashchenko, and A. Kedrovskaya, "Preparation and properties of nanocellulose from peracetic flax pulp," *Journal of Scientific Research and Reports*, vol. 16, no. 1, pp. 1–10, 2017.
- [19] V. A. Barbash, O. V. Yaschenko, and V. O. Opolsky, "Effect of hydrolysis conditions of organosolv pulp from kenaf fibers on the physicochemical properties of the obtained nanocellulose," *Theoretical and Experimental Chemistry*, vol. 54, no. 3, pp. 193–198, 2018.
- [20] A. Płazek, F. Dubert, P. Kopeć et al., "In vitro-propagated *Miscanthus × giganteus* plants can be a source of diversity in terms of their chemical composition," *Biomass and Bioenergy*, vol. 75, pp. 142–149, 2015.
- [21] N. Brosse, A. Dufour, X. Meng, Q. Sun, and A. Ragauskas, "Miscanthus: a fast-growing crop for biofuels and chemicals production," *Biofuels Bioproducts & Biorefining*, vol. 6, no. 5, pp. 580–598, 2012.
- [22] E. Cudjoe, M. Hunsen, Z. Xue et al., "Miscanthus giganteus: a commercially viable sustainable source of cellulose nanocrystals," *Carbohydrate Polymers*, vol. 155, pp. 230–241, 2017.
- [23] TAPPI, *Test Methods*, Georgia, Tappi Press, Atlanta, 2004.
- [24] M. Poletto, H. O. Júnior, and A. Zattera, "Native cellulose: structure, characterization and thermal properties," *Materials*, vol. 7, no. 9, pp. 6105–6119, 2014.
- [25] R. A. Ilyas, S. M. Sapuan, M. R. Ishak, and E. S. Zainudin, "Effect of delignification on the physical, thermal, chemical, and structural properties of sugar palm fibre," *BioResources*, vol. 12, no. 4, pp. 8734–8754, 2017.
- [26] G. B. Paschoal, C. M. O. Muller, G. M. Carvalho, C. A. Tischer, and S. Mali, "Isolation and characterization of microfibrillated cellulose from oat hulls," *Química Nova*, vol. 38, no. 4, pp. 478–482, 2015.
- [27] V. A. Barbash, O. V. Yaschenko, S. V. Alushkin, A. S. Kondratyuk, O. Y. Posudievsky, and V. G. Koshechko, "The effect of mechanochemical treatment of the cellulose on characteristics of nanocellulose films," *Nanoscale Research Letters*, vol. 11, no. 1, p. 410, 2016.
- [28] A. B. Fall, A. Burman, and L. Wagberg, "Cellulosic nanofibrils from eucalyptus, acacia and pine fibers," *Nordic Pulp & Paper Research Journal*, vol. 29, no. 1, pp. 176–184, 2014.
- [29] A. B. Reising, R. J. Moon, and J. P. Youngblood, "Effect of particle alignment on mechanical properties of neat cellulose nanocrystal films," *Journal of Science & Technology for Forest Products and Processes*, vol. 2, no. 6, pp. 32–41, 2012.
- [30] R. Hashaikeh and H. Abushammala, "Acid mediated networked cellulose: preparation and characterization," *Carbohydrate Polymers*, vol. 83, no. 3, pp. 1088–1094, 2011.
- [31] M. Roman and W. Winter, "Effect of sulfate groups from sulfuric acid hydrolysis on the thermal degradation behavior of bacterial cellulose," *Biomacromolecules*, vol. 5, no. 5, pp. 1671–1677, 2004.



**Hindawi**  
Submit your manuscripts at  
[www.hindawi.com](http://www.hindawi.com)

